3D-QSAR of PET Agents for Imaging β-Amyloid in Alzheimer's Disease

Mi Kyoung Kim, Il Han Choo,† Hyo Sun Lee, Jong Inn Woo,† and Youhoon Chong*

*Department of Bioscience and Biotechnology, Konkuk University, Seoul 143-701, Korea. *E-mail: chongy@konkuk.ac.kr*
†Department of Neuropsychiatry, Seoul National University College of Medicine, Seoul 110-744, Korea
Received May 19, 2007

Key Words : PET, β-Amyloid, 3D-QSAR, CoMSIA

Accumulation of excess senile plaques (β-amyloid, Aβ-plaques) in the brain is strongly associated with the pathogenesis of Alzheimer's disease (AD).[1] While there are no definitive treatments available to affect a cure of AD, much recent interest has been given to the development of anti-amyloid therapies aimed at halting and reversing Aβ-deposition and, thus, monitoring of the therapeutic efficacy would greatly benefit from methods for the *in vivo* detection and quantification of Aβ-deposits in the brain.[2]

Several groups have reported a series of potential imaging agents for the *in vivo* imaging of Aβ-plaques with positron emission tomography (PET) or single-photon emission computed tomography (SPECT). However, to our knowledge, no three dimensional structure activity relationship (3D-QSAR) studies on PET ligands have been published so far with the exception of CoMFA/CoMSIA study on serotonin transporter (SERT) ligands.[3] and the aim of the present study was to quantitatively investigate structure-activity relationships (SAR) of PET ligands with regard to the future development of potential new PET radiotracers by using Comparative Molecular Field Analysis (CoMFA) and Comparative Molecular Similarity Indices Analysis (CoMSIA).

In this study, we constructed a 3D-QSAR model with several PET ligands such as ThioT analogues and stilbene derivatives, which could be applied to predict binding affinity of the structurally related compounds against Aβ-plaques. From the literature, binding affinity data of 62 ThioT derivatives[4,5] and 11 stilbene derivatives[6] were obtained which were used for model building (Fig. 1). At first, the 73 compounds obtained from the literature were divided into two groups: 63 compounds as training set and the other 10 compounds as test set. The training set was used to build 3D-QSAR models with CoMFA and CoMSIA methods, while the test set was used to validate the 3D-

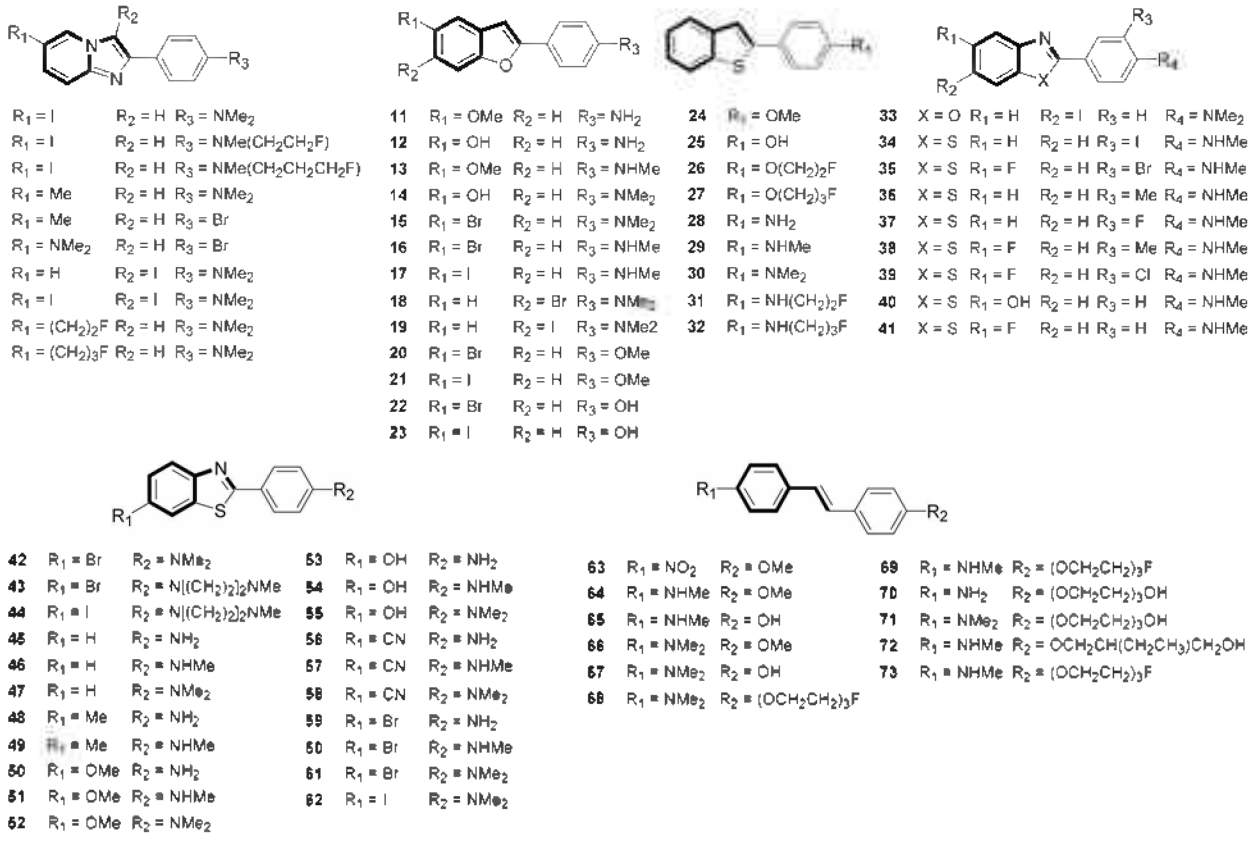

Figure 1. ThioT and stilbene derivatives used for 3D-QSAR study. Fragments used for structural alignment are represented in bold lines.

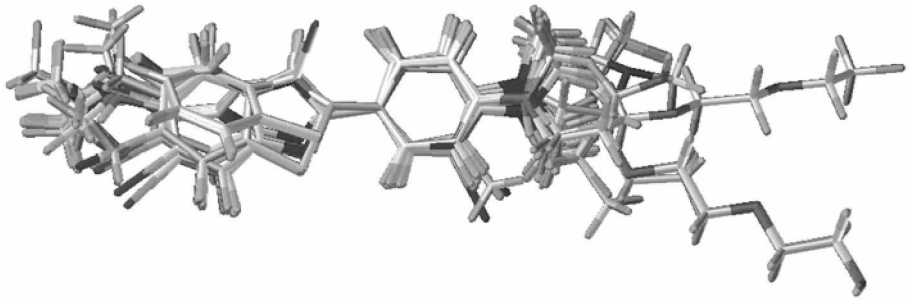

Figure 2. Structural alignment of ThioT and stilbene derivatives around the common substructure PhCH=CH.

Table 1. PLS analysis on PET ligands

Model	Cross-Validated			Non-cross-validated			Fraction %				
	q^2	SEP	N	r^2	SEE	F	S[d]	E[d]	H[d]	D[d]	A[d]
CoMFA	0.631	0.520	5	0.926	0.234	148.45	0.347	0.653	–	–	–
CoMSIA$_{se}$[a]	0.525	0.589	4	0.839	0.343	78.024	0.181	0.819	–	–	–
CoMSIA$_{da}$[b]	0.508	0.600	4	0.876	0.304	83.236	0.730	0.270	–	–	–
CoMSIA$_{all}$[c]	0.654	0.503	4	0.900	0.270	135.69	0.204	0.051	0.259	0.149	0.337

q^2-leave one out (LOO) cross-validated correlation coefficient. SEP-standard error of prediction, N-optimum number of components, r^2-non-cross-validated correlation coefficient, SEE-standard error of estimate, F-F-test value. [a]s = steric field, e = electrostatic field. [b]d = hydrogen bond donor, a = hydrogen bond acceptor. [c]all = steric + electrostatic + hydrogen bond donor + hydrogen bond acceptor + hydrophobic. [d]S = steric, E = electrostatic, H = hydrophobic, D = hydrogen bond donor, A = hydrogen bond acceptor

QSAR model. Finally, the contour plots of CoMFA and CoMSIA were analyzed to provide helpful information on how to improve the binding affinity of ThioT derivatives by structural modifications.

All calculations were carried out on a linux enterprise operating system using molecular modeling software package SYBYL v 7.2. All compounds were constructed by the Sketch module in SYBYL base and assigned with MMFF94s charges. For more flexible compounds, systematic searches were performed with an interval of 10° on every rotatable bond to ensure their lowest energy conformations. Finally, they were minimized with MMFF94s force field. The most crucial step in performing 3D-QSAR is to determine the bioactive conformations of the compounds so that all compounds could be aligned together. In this study, the styrene moiety [PhC=X (X = C or N)] commonly found in the ThioT and stilbene derivatives was used as the substructure for alignment. The compound PIB (**54**) was used as a template for structural alignment from the alignment facility in SYBYL, and 63 training set molecules and 10 test set molecules were all aligned together (Fig. 2).

With the structure-based ligand alignment in hand, we attempted 3D-QSAR study by using CoMFA[7,8] as well as CoMSIA[9,10] method with grid spacing of 2.0 Å. As usual, PLS (partial least squares) method was used to establish and validate 3D-QSAR. The K_i values were converted into pK_i ($-\log K_i$) to describe the binding affinities. CoMFA was set at standard values, with a sp^3 carbon atom with one positive charge used to probe steric and electrostatic fields. The standard cutoff value was set to 30 kcal/mol. LOO (leave-one-out) cross-validation method was used to evaluate the initial model. The cross-validated coefficient q^2 was calculated, the optimum number of components was then given, and CoMFA model was finally derived corresponding to the optimum number. The column filtering box was kept unchecked during all operations (Table 1).

The basic principle of CoMSIA is the same as that of CoMFA, but CoMSIA includes some additional descriptors such as hydrophobicity, hydrogen bond donor and hydrogen bond acceptor. As in the CoMFA model, the same regression analysis was used for CoMSIA field energies, and the results obtained from the PLS analysis are also summarized in Table 1.

The CoMFA model with 63 molecules in the training set is consequently a clearly statistically significant model showing a cross-validated q^2-value of 0.631 at 5 components (Table 1). This analysis was used for the final non-cross-validated run, giving a good correlation coefficient (r^2 value of 0.926) (Table 1). Using steric, electrostatic, hydrophobic, and hydrogen bond donor and acceptor properties as descriptors, CoMSIA analysis was performed and the results are also listed in Table 1. The best q^2 was found using all five different descriptor variables, which demonstrates that these variables are necessary to describe the interaction mode of the PET ligands with Aβ-plaques. The CoMSIA model with a cross-validated q^2 of 0.654 for 4 components and a conventional r^2 of 0.900 was obtained (Table 1). These data demonstrate that the CoMSIA model is stable and statistically significant and it should be noted that, due to the use of less components than CoMFA model, the CoMSIA model has reduced risk of overtraining the system. The corresponding field distributions of these five descriptor variables were 20.4, 5.1, 25.9, 14.9, and 33.7%, respectively, which indicates that steric rather than electrostatic and H-bond acceptor

Table 2. Predicted binding affinities (PBA) versus experimental binding affinities (EBA, pK_i) and residuals (d) by CoMFA and CoMSIA

	EBA	CoMFA		CoMSIA			EBA	CoMFA		CoMSIA			EBA	CoMFA		CoMSIA	
		PBA	d	PBA	d			PBA	d	PBA	d			PBA	d	PBA	d
1	7.82	7.63	0.19	7.28	0.54	**26**	9.17	8.94	0.23	9.06	0.12	**51**	8.31	8.57	−0.26	8.19	0.12
2	7.57	7.19	0.38	7.33	0.24	**27**	9.19	9.15	0.04	9.11	0.08	**52**	8.72	8.86	−0.14	8.49	0.23
3	7.40	7.36	0.04	7.27	0.13	**28***	8.37	8.75	−0.38	8.74	−0.37	**53***	7.34	7.80	−0.46	7.61	−0.27
4*	6.62	7.43	−0.81	6.98	−0.37	**29***	9.55	8.89	0.66	9.01	0.54	**54**	8.37	8.22	0.15	7.96	0.40
5	6.20	6.30	−0.10	6.45	−0.26	**30**	8.97	9.21	−0.23	9.17	−0.20	**55**	8.36	8.58	−0.22	8.26	0.10
6	6.47	6.58	−0.11	6.41	0.06	**31**	8.81	9.05	−0.25	9.13	−0.32	**56**	7.19	7.29	−0.10	7.37	−0.18
7	5.70	5.66	0.04	5.93	−0.23	**32**	9.14	9.21	−0.07	9.16	−0.02	**57**	8.07	7.68	0.39	7.72	0.34
8	5.70	5.75	−0.05	5.90	−0.20	**33***	9.10	9.06	0.04	8.98	0.12	**58**	7.96	8.02	−0.06	8.02	−0.06
9	6.75	6.93	−0.18	6.93	−0.17	**34**	8.64	8.86	−0.22	8.92	−0.28	**59**	8.14	7.82	0.32	8.19	−0.05
10	7.32	7.46	−0.15	7.13	0.18	**35**	8.89	8.67	0.22	8.37	0.52	**60***	8.77	8.21	0.56	8.54	0.23
11	8.64	8.93	−0.29	8.63	0.01	**36**	8.36	8.41	−0.05	8.32	0.04	**61**	8.54	8.58	−0.04	8.84	−0.31
12	7.94	8.16	−0.23	8.45	−0.51	**37**	8.17	7.98	0.19	8.21	−0.04	**62**	9.05	8.70	0.34	8.85	0.20
13*	8.89	8.92	−0.04	8.81	0.08	**38***	8.08	8.67	−0.59	8.34	−0.27	**63**	6.82	6.94	−0.12	6.71	0.12
14	8.55	8.78	−0.22	8.66	−0.11	**39**	8.47	8.26	0.21	8.20	0.27	**64**	8.92	8.64	0.28	8.59	0.33
15	8.80	8.93	−0.14	8.89	−0.10	**40**	8.42	8.15	0.27	8.04	0.38	**65***	8.22	8.61	−0.39	8.27	−0.04
16	8.57	8.65	−0.08	8.88	−0.31	**41**	7.91	8.33	−0.43	8.34	−0.43	**66**	8.89	8.90	−0.01	8.69	0.19
17	8.96	8.54	0.42	8.94	0.02	**42**	8.72	8.81	−0.09	8.69	0.04	**67**	8.66	8.91	−0.25	8.45	0.20
18	9.22	9.37	−0.15	9.18	0.04	**43**	8.80	8.61	0.18	8.66	0.14	**68**	8.60	8.38	0.22	8.54	0.06
19	9.40	9.37	0.03	9.37	0.03	**44**	8.27	8.47	−0.20	8.82	−0.55	**69**	8.00	8.26	−0.26	8.27	−0.27
20	8.89	8.51	0.38	8.66	0.23	**45**	7.43	7.69	−0.26	7.86	−0.43	**70**	7.04	7.61	−0.57	7.50	−0.45
21	8.38	8.41	−0.04	8.71	−0.34	**46**	7.96	8.01	−0.05	8.21	−0.25	**71**	8.66	8.16	0.50	8.29	0.37
22	8.05	8.17	−0.12	8.32	−0.28	**47**	8.40	8.35	0.04	8.50	−0.11	**72**	8.30	8.24	0.07	8.15	0.15
23	8.19	8.07	0.12	8.38	−0.19	**48**	8.02	7.98	0.04	7.98	0.04	**73***	8.17	8.12	0.05	8.17	0.00
24	9.40	8.95	0.44	8.93	0.47	**49**	8.00	8.24	−0.24	8.31	−0.31						
25	8.52	8.60	−0.08	8.56	−0.05	**50**	8.15	8.12	0.04	7.83	0.33						

*test set compounds

rather than H-bond donor contribute more to the final CoMSIA model, and thus, these fields play crucial roles in determining the binding affinity of the PET ligands to the target protein. Predicted binding affinities, given as pK_i values, and the residuals of the final non cross-validated CoMFA as well as CoMSIA models are shown in Table 2, and the plot of actual pK_i values versus predicted pK_i is shown in Figure 3.

The ultimate test for the usefulness of a 3D-QSAR model is predicting the activity of new compounds that are not included in the dataset that is used to obtain the model. To validate the stability and predictive ability of our 3D-QSAR model, 10 PET ligands (compounds **4**, **13**, **28**, **29**, **33**, **38**, **53**, **60**, **65**, **73**) that were not included in the construction of CoMFA and CoMSIA models are selected as the test set. The binding affinities of the test set molecules were predicted reasonably well (residuals from 0.04 to 0.81 for CoMFA model and 0.04 to 0.54 for $CoMSIA_{all}$ model) and the results were also summarized in Table 2 and Figure 3. The predictive performance of models on the test set was estimated by predictive r^2 value (r^2_{pred}). The predictive performances of CoMFA and $CoMSIA_{all}$ model on the test were $r^2_{pred} = 0.74$ and $r^2_{pred} = 0.93$, respectively, which indicated that the CoMSIA model was more reliable and able to predict biological activity of new derivatives more accurately.

Graphical representations of CoMSIA maps obtained by

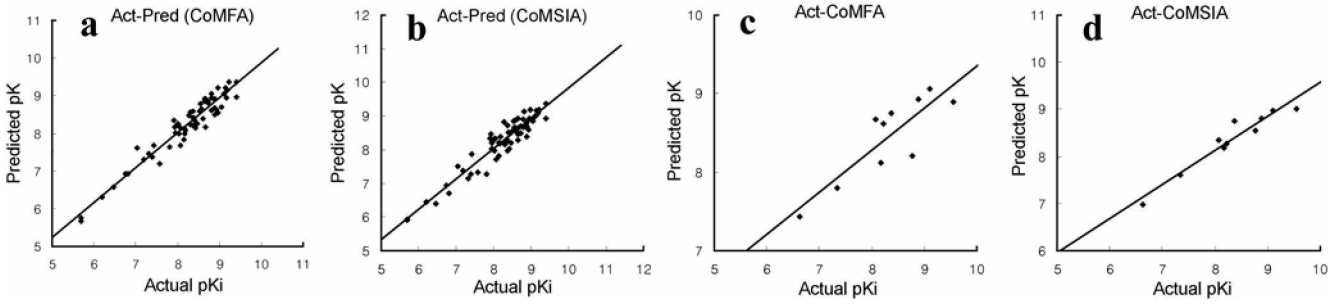

Figure 3. Plot of observed pK_i versus conventional fit predictions (predicted activity) of training set (a: CoMFA model, b: CoMSIA model) and test set (c: CoMFA model, d: CoMSIA model).

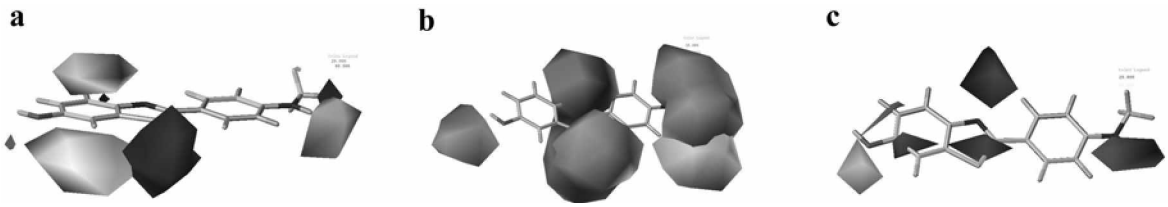

Figure 4. CoMSIA Contour plots: PIB (**54**) is depicted as a reference molecule: (a) $CoMSIA_{se}$: green and blue contours predict that the binding affinity is enhanced by bulky substituent and positive charge, respectively, whereas yellow contours predict less bulky group is favored for activity, (b) $CoMSIA_{da}$: orange contours predict H-bond acceptors enhance activity and cyan contours predict H-bond donor enhance activity; (c) $CoMSIA_{h}$: Yellow contours predict hydrophobic substituents enhance activity whereas purple contours predict hydrophobic substituents decrease activity.

the field type "stDev*coeff" are displayed in Figure 4. The contour maps were superimposed on the compound PIB (**54**) shown as a capped stick. The $CoMSIA_{se}$ (Fig. 4a) contour plots show green and yellow contour plots over and beneath the benzothiazole ring, respectively, which means that the coplanarity of the PET ligands would be the key for high binding affinity to the target protein. Thus, substitution at the α-position of the phenyl ring of **54** (Fig. 4a), which would result in distortion of the molecule, would not be beneficial to the binding affinity. On the other hand, significant preferences for positive electrostatic interaction around the sulfur atom of the benzothiazole ring system could be found, and positively charged groups or electron-donating substituents may increase the binding affinity of ThioT derivatives to the target protein by taking advantage of the electrostatic nature of the environment at this position. The contour maps of the hydrogen bond donor and acceptor fields describe the spatial arrangement of favorable hydrogen bond interactions, and these interactions are heavily focused on the donor groups of the target protein (Fig. 4b). The orange contours that are observed around the thiazole ring, phenolic hydroxyl group and anilinic amino group indicate favorable hydrogen bonds to donor groups in the target protein. In the hydrophobic maps of CoMSIA (Fig. 4c), the yellow and purple contours represent the regions of favorable and unfavorable hydrophobic interactions, respectively. As was shown in the steric and electrostatic maps (Fig. 4a), hydrophobic interaction above and beneath the benzothiazole ring is detrimental for binding affinity. Also, terminal anilinic amino group has a strong preference for monoalkyl substituents for high binding affinity. The only site available for beneficial substitution with hydrophobic group is expected to be around the position corresponding to the phenolic OH group of **54**.

Acknowledgments. This work was supported by grant KRF-2006-331-C00176 from the Korea Research Foundation, Republic of Korea (MOEHRD, Basic Research Promotion Fund) and by grants from Biogreen 21 (Korea Ministry of Agriculture and Forestry). MKK and HSL are supported by the second Brain Korea 21.

References

1. Hardy, J.; Selkoe, D. J. *Science* **2002**, *297*, 353.
2. Nordberg, A. *Lancet Neurol.* **2004**, *3*, 519.
3. (a) Wellsow, J.; Machulla, H.-J.; Kovar, K.-A. *Quant. Struct.-Act. Relat.* **2002**, *21*, 577. (b) Wellsow, J.; Kovar, K.-A. *J. Pharm. Pharmaceut. Sci.* **2002**, *5*, 245.
4. (a) Klunk, W. E.; Wang, Y.; Huang, G. F.; Debnath, M. L.; Holt, D. P.; Mathis, C. A. *Life Sci.* **2001**, *69*, 1471. (b) Mathis, C. A.; Wang, Y.; Holt, D. P.; Huang, G.-F.; Debnath, M. L.; Klunk, W. E. *J. Med. Chem.* **2003**, *46*, 2740. (c) Zhuang, Z. P.; Kung, M. P.; Hou, C.; Skovronsky, D. M.; Gur, T. L.; Plossl, K.; Trojanowski, J. Q.; Lee, V. M.; Kung, H. F. *J. Med. Chem.* **2001**, *44*, 1905.
5. (a) Cai, L.; Chin, F. T.; Pike, V. W.; Toyama, H.; Liow, J.-S.; Zoghbi, S. S.; Modell, K.; Briard, E.; Shetty, H. U.; Sinclair, K.; Donohue, S.; Tipre, D.; Kung, M.-P.; Dagostin, C.; Widdowson, D. A.; Green, M.; Gao, W.; Herman, M. M.; Ichise, M.; Innis, R. B. *J. Med. Chem.* **2004**, *47*, 2208. (b) Ono, M.; Kawashima, H.; Nonaka, A.; Kawai, T.; Haratake, M.; Mori, H.; Kung, M.-P.; Kung, H. F.; Saji, H.; Nakayama, M. *J. Med. Chem.* **2006**, *49*, 2725. (c) Zhuang, Z.-P.; Kung, M.-P.; Wilson, A.; Lee, C.-W.; Plossl, K.; Hou, C.; Holtzman, D. M.; Kung, H. F. *J. Med. Chem.* **2003**, *46*, 237. (d) Zhuang, Z.-P.; Kung, M.-P.; Hou, C.; Plossl, K.; Skovronsky, D.; Gur, T. L.; Trojanowski, J. Q.; Lee, V. M.-Y.; Kung, H. F. *Nucl. Med. Biol.* **2001**, *28*, 887. (e) Ono, M.; Kung, M.-P.; Hou, C.; Kung, H. F. *Nucl. Med. Biol.* **2002**, *29*, 633. (f) Ono, M.; Wilson, A.; Nobrega, J.; Westaway, D.; Verhoeff, P.; Zhuang, Z.-P.; Kung, M.-P.; Kung, H. F. *Nucl. Med. Biol.* **2003**, *30*, 565. (g) Henriksen, G.; Hauser, A.; Westwell, A. D.; Yousefi, B. H.; Schwaiger, M.; Drzezga, A.; Wester, H.-J. *J. Med. Chem.* **2007**, *50*, 1087. (h) Chang, Y. S.; Jeong, J. M.; Lee, Y.-S.; Kim, H. W.; Rai, B. G.; Kim, Y. J.; Lee, D. S.; Chung, J.-K.; Lee, M. C. *Nucl. Med. Biol.* **2006**, *33*, 811. (i) Zeng, F.; Southerland, J. A.; Voll, R. J.; Votaw, J. R.; Williams, L.; Ciliax, B. J.; Levey, A. I.; Goodman, M. M. *Bioorg. Med. Chem. Lett.* **2006**, *16*, 3015.
6. Zhang, W.; Kung, M.-P.; Oya, S.; Hou, C.; Kung, H. F. *Nucl. Med. Biol.* **2007**, *34*, 89.
7. Cramer, M.; Cramer, R. D.; Jones, D. M. *J. Am. Chem. Soc.* **1988**, *110*, 5959.
8. Kim, J.; Lee, M.; Kang, S.-Y.; Park, J.; Lim, Y.; Koh, D.; Park, K. H.; Chong, Y. *Bull. Korean Chem. Soc.* **2006**, *27*, 1025.
9. Klebe, G.; Abraham, U.; Mietzner, T. *J. Med. Chem.* **1994**, *37*, 4130.
10. Kim, J.; Han, J. H.; Chong, Y. *Bull. Korean Chem. Soc.* **2006**, *27*, 1919.